An Electrophoresis-Aided Biomineralization System for Regenerating Dentin-and Enamel-Like Microstructures for the Self-Healing of Tooth Defects

Xiao-Ting Wu, [†] ***Quan-Li Li,*** [†,*] ***Ying Cao,*** [‡] ***May Lei Mei,*** [‡] ***Jia-Long Chen,*** [†] ***Chun Hung Chu*** [‡,*]

†College & Hospital of Stomatology, Anhui Medical University, Hefei, China

‡ Faculty of Dentistry, University of Hong Kong, Hong Kong, China

Key words *: Dentin, Enamel, Remineralization, Collagen, Electrophoresis, Biomineralization*

Corresponding Author

*E-mail: chchu@hku.hk (C.H.C.). ql-li@126.com (Q.-L.L.)

Tel: (+) 852-28590287 (C.H.C.). 86-551-65118677 (Q.-L.L.)

Fax: (+) 852-25599013 (C.H.C). 86-551-5121527 (Q.-L.L.)

Abstract

The time required by the available biomimetic remineralization protocols to regenerate calcified dentin collagen fibrins and enamel prism-like tissue on dentin is long and takes a few weeks. This study aimed to develop a novel electrophoresis-aided calcium and phosphate hydrogel system to shorten the time for the biomimetic remineralization on dentin. An acid-etched human dentin slice was placed between 2 layers of freshly prepared agarose hydrogel which contained calcium chloride and disodium hydrogen phosphate, respectively. They were put in a polyether tube and electrophoresis was delivered by applying a constant direct current to the terminal of the 2 hydrogels for 12 hours. After the treatment, the precipitates formed on the dentin slices were characterized using Fourier transform infrared spectroscopy, X-ray diffraction, scanning electron microscopy, transmission electron microscopy and selected area electron diffraction. The results showed that the precipitates formed were hydroxyapatites. The demineralized dentin collagen matrix was remineralized with intrafibrillar and interfibrillar hydroxyapatites mimicking structure of calcified dentin collagen matrix. The precipitated hydroxyapatites were densely-packed needle-like crystals and occluded the exposed dentinal tubules. The morphology demonstrated enamel-like tissue precipitation on remineralized dentin surface. In conclusion, this study developed an electrophoresis-aided system to shorten the time for biomimetic mineralization of dentine by regenerating the natural dentin microstructure of calcified collage fibrils and formation of enamel prism-like tissue covering dentin surface

1. INTRODUCTION

Dentin comprises the main body of teeth, and its outer surface is covered by enamel and its inner surface forms a pulp cavity full of dental pulp soft tissue. Enamel, the exterior layer of teeth is the hardest and most highly mineralized human tissue. It loads the mastication stresses and protects the dentin-pulp complex. Tooth wear such as abrasion, attrition and dental erosion result from enamel loss and exposed dentin can give rise to dentin hypersensitivity. Although damaged dental hard tissue may be self-repaired by remineralization in the presence of saliva, the loss of dental hard tissue cannot be regenerated. Recently, the cell-free biomimetic mineralization strategy has being managed to regenerate tooth-like microstructure *in vitro*. It has provided the potentials of repairing the tooth defects by self-healing, and it is much more desirable for dentistry clinic.

Enamel is composed of 96% inorganic mineral of hydroxyapatite (HA) crystals. HA crystals assemble into prism structure, and these prisms are tightly packed in an organized pattern to form a special enamel microstructure. Each prism is approximately 4 μm to 8 μm in diameter and is made up of HA crystals bundled in parallel with each other, with each crystal having a cross-section of 25 nm to100 nm and a variable length of 100 nm to 100 μm or more along the c-axis. Various methods have been proposed to regenerate enamel-like prism structure, such as hydrothermal methods,[1] extremely acid calcium phosphate paste containing hydrogen peroxide and phosphoric acid,[2] surfactants,[3, 4] ethylenediaminetetraacetic acid (EDTA),[5] nano-HA and glutamic acid,[6] amelogenin,[7-9] gelatin,[10] polyethylene oxide and polyacrylamide.[11] All these mentioned methods regenerated enamel-like tissue on demineralized enamel surface but not on dentin surface.

Structurally, the basic microstructure of dentin comprises calcified collagen matrix. It contains approximately 70% by weight inorganic mineral of HA, 20% organic matrix and 10% water. The main organic substance of dentin is type I collagen, which self-assembles into fibrils to form the collagen matrix scaffolds. The inorganic mineral HA crystals can be classified as intrafibrillar and interfibrillar crystallites. Intrafibrillar crystallites are deposited with their *c*-axis aligned in parallel to the collagen fibrils and thus are oriented along the collagen fibrils.

Interfibrillar crystallites are deposited between the collagen fibers and hence they are also referred as extrafibrillar crystallites. Calcified collagen fibrils, especially the intrafibrillar mineralization of collagen fibrils, are believed to be responsible for the biomechanical properties of dentin and protecting collagen fibers from degradation.[12, 13] Thus, it is the essential to form intrafibrillar HA for remineralization of dentin collagen matrix to regenerate the dentin microstructure of calcified collagen fibrins.

Remineralization of dentin collagen fibrils is more complicated and difficult than remineralization of enamel.[14] The role of collagen matrix in apatite mineralization still remains a topic of debate. However, more evidence supports the notion that dentinal collagen matrix is ineffective for intrafibrillar mineralization. Non-collagenous proteins play an important role in initiating and regulating HA nucleation and growth to induce collagen mineralization, especially intrafibrillar mineralization.[15-17] Several methods without using non-collagenous protein analogues such as those using casein phosphopeptide-amorphous calcium phosphate, colloidal nano-β-tricalcium phosphate and bioactive glass particles, polydopamine, and agarose gel, didn't demonstrated the success in reproducing the structural hierarchy of apatite deposition within the collagen matrices.[18-22]

On the contrary, the biomimic of non-collagenous protein strategy such as using polyacrylic acid and polyvinylphosphonic acid, sodium trimetaphosphate, tripolyphosphate, oligopeptides inspired by non-collagenous proteins, polymer-induced liquid mineral precursors (PILP), and poly(amido amine) dendrimer, have demonstrated intrafibrillar mineralization.[23-28] However, none has declared forming enamel-like tissue on remineralized dentin surface.

It is noteworthy that the rate of precipitate growth is very slow in the aforementioned methods, which limits their clinical application. Tay et al reported that mineralization in a 5 μm demineralized region started at 2 weeks, and complete remineralization was achieved at 8 weeks.[14] Busch reported that the rate of enamel-like tissue regeneration was approximately 500 nm/day with the gelatin hydrogel model.[10]

In gist, regeneration of tooth-like tissue by biomimetic mineralization are challenging because remineralization of dentin collagen fibrils to duplicate the calcified collagen fibrils hierarchical structure is more difficult than remineralization of enamel. Moreover, the time of the mineralization is very long. There is no study so far reported regeneration of enamel-like tissue on remineralized dentin surface.

Electrophoresis can transport ions more rapidly than diffusion in a gel or solution. It also enables ion migration in a specific direction. Electrophoresis has been used to accelerate HA formation in hydrogels to synthesize hybrid materials.[29, 30] We created a calcium and phosphate agarose hydrogel system to remineralize dentin and enamel in the absence of non-collagenous protein analogues.[22, 31] In the present study, we aimed to shorten the time by electrophoresis to remineralize the demineralized dentin and to cover the dentin surface with regenerated enamel-like tissue in an agarose hydrogel system.

2. MATERIALS AND METHODS

2.1. Dentin slice preparation

This study was approved by The University of Hong Kong/Hospital Authority Hong Kong West Cluster Institutional Review Board (IRB UW10-210). Patients who required extraction of their sound molars invited to donate their extracted molars. The soft tissue attached to the molars was removed by a scalpel. The molars were disinfected with 3% sodium hypochlorite and rinsed with phosphate-buffered saline. Dentin slices of 2 mm thickness were prepared perpendicular to the longitudinal axis of the tooth using a low-speed diamond saw (IsoMet Low Speed Saw, Buehler, Lake Bluff, Illinois, USA). Silicon carbide papers were used for polishing. They were ultrasonically cleaned and stored at 4ºC in deionized water.

2.2. Agarose gels preparation

The $CaCl_2$ agarose gel was prepared by mixing agarose powder (Regular Agarose G-10, BIOWEST, Nuaillé, France) (1.0 g) in 100 mL of 0.13 M $CaCl_2$ solution ($CaCl_2 \cdot 2H_2O$, Sigma-Aldrich, St. Louis, MO, USA). The Na_2HPO_4 agarose gel with 500 ppm fluoride was prepared by mixing agarose powder (1.0 g) in 100 mL of 0.26 M Na_2HPO_4 (Sigma-Aldrich, St.

Louis, MO, USA) solution containing 500 ppm fluoride (Sigma-Aldrich, St. Louis, MO, USA). The pH value was adjusted to 6.5 using 0.1 M NaOH and 0.1 M HCl. The mixtures were allowed to swell for 30 min and then heated to 100ºC to completely dissolve the agarose.

2.3. Remineralization in agarose gel aided by electrophoresis

The dentin slices were etched with 37% H_3PO_4 solution for 30 s to create demineralized dentin surface with exposed collagen matrix. The electrophoresis device consists of a two-way horizontal polyether tube, 2 plastic cells and 2 graphite electrodes (DYY-10C Electrophoresis, Liuyi Instrument Factory, Beijing, China) (Figure 1). The $CaCl_2$ agarose gel and the Na_2HPO_4 agarose gel are put into the two sides of the tube separated by the etched dentine slice. The tube was then connected to the plastic cells. Electrodes were set into the bottom of the cells, which were filled with 0.9% NaCl solution to enhance the electrical conductivity. The electric current was maintained constant at 20 mA during electrophoresis. The gels and NaCl solution were refreshed every 2 hours which was defined as a cycle of mineralisation. The dentin slice was cleaned ultrasonically for 2 min after each cycle. The sample was taken out after 2, 4 and 6 cycles for assessment and characterization.

2.4. Characterizing the dentine slices after remineralization

2.4.1. XRD and FTIR evaluation of the composition and structure of the remineralized dentin surface

The composition of precipitates formed on the etched dentin slice after 6 cycles of mineralization was evaluated by X-ray diffraction (XRD) (X'Pert Pro, Philips Almelo, Netherlands), and diffuse-reflection Fourier transform infrared spectroscopy (DR-FTIR) (Nicolet 8700, Thermo Scientific Instrument Co, Friars Drive Hudson, NH, USA). For comparison, dentin slice without acid-etching and acid-etched dentin slice without electrophoresis were studied as control.

2.4.2. SEM evaluation of the morphology and location of the precipitated HA crystals

The dentin slices were dehydrated with a series of ethanol and dried in a critical-point evaporator before sputter-coated with gold for SEM analysis. The morphology and site of the

precipitates were evaluated by field emission scanning electron microscopy (FE-SEM, Sirion 200, FEI Co, Hillsboro, OR, USA, or S4800, Hitachi High Technologies America, Inc., Dallas, USA).

2.4.3. TEM evaluation of intrafibrillar mineralization formation

The surface of the dentin slice after 4 cycles of mineralization and acid-etched dentin slice without remineralization was scratched using a probe and the crumbs collected were smeared onto a copper grid for analysis with transmission electron microscopy (TEM) (Tecnai G2 20, FEI Co., Hillsboro, OR, USA). Bright-field and selected area electron diffraction (SAED) modes were used with no staining preparation.

3. RESULTS

3.1. XRD and FTIR evaluation of the composition and structure of the remineralized dentin surface

XRD spectra confirmed that the precipitates on the dentin slices were HA. Spectrum (a) in Figure 2 shows XRD patterns of the crystals grown on the dentin surface after 6 cycles of mineralization in the agarose hydrogel microenvironment aided by electrophoresis. The diffraction peaks (002) at 2θ=25.8, (211) at 2θ=31.9, (112) at 2θ=32.3, and (300) at 2θ=33.0 corresponded well to the expected peaks for HA. The ratio of the diffraction intensity of the c-axis (002) reflection to the diffraction intensity of the a-axis (300) reflection in the slice treated with electrophoresis was considerably greater than that of the slice without acid-etching (spectrum b). The result suggested that the HA precipitates were oriented along its c-axis. Distinct diffraction peaks around 2θ = 31.9 to 33.0 could be identified in the spectrum indicating the good crystallinity of the HA. These diffraction peaks were difficult to identify in spectrum of acid-etched or untreated dentin specimens. These findings were consistent with the observations in the SEM as shown in Figure 5.

The FTIR analysis demonstrated compositional change on the dentin surface after mineralization (Figure 3). The FTIR spectrum of the acid-etched dentin surface (c – blue line)

was characterized by the peaks corresponding to collagen and few HA peaks were observed before mineralization. The peaks at approximately 1633 cm^{-1} and 1528 cm^{-1} represented amide I and amide II contributed by dentin collagen matrix, respectively. In contrast, the FTIR spectrum of the remineralized dentin surface was characterized predominantly by HA peaks (a- red line). Few collagen peaks were visible. A distinct $-PO_4$ band in the FTIR spectra of the remineralized slices showed remarkable P−O splitting asymmetric stretching (υ_3) at 1050 (υ_{3-1}) cm^{-1} and 1110 (υ_{3-2}) cm^{-1}, and P−O splitting bending (υ_4) at 604 (υ_{4-1}) cm^{-1} and 569 (υ_{4-2}) cm^{-1}. The intensities of the amide peaks corresponding to amide I and amide II were significantly reduced.

Regarding the FTIR spectrum of the dentin surface without acid-etching (b- black line), the $-PO_4$ band peaks was present in relative weak and vague appearance comparing to the remineralized samples. It suggested that the size of HA crystal was smaller, and the crystallinity was lower than of the precipitate HA. The observation was also corresponded well to the XRD spectrum. The intensities of the amide peaks were reduced in the spectrum of the dentin exposed to the mineralization system. The intensity of the PO_4 band was enhanced compared with the spectrum of acid-etched dentin. These differences indicated that more HA were deposited on the collagen fiber surface after electrophoresis.

3.2. SEM evaluation of the morphology and location of the precipitated HA crystals

3.2.1 Enamel-like tissue forming on dentin surface

SEM evaluation of the acid-etching dentin slice surface showed that the dentin collagen fibers were demineralized and the collagen matrix was exposed (Figure 4a). The dentinal tubules on the dentine surface became patent after acid-etching. The diameter of the dentinal tubule in the demineralized dentin was enlarged (Figure 4b). The zone of demineralization was approximately 5 μm in depth. In contrast, needle-shaped HA crystals were observed on the remineralized dentin slices. The needle-shaped HA crystals grew with time from the dentin surface and the wall of dentinal tubule, and they gradually covered the dentinal tubules. The needle-shaped HA crystals were densely packed together after 6 cycles of mineralization. They completely covered the underlining dentin tissue and the dentinal tubules (Figure 4 c to h). The

densely packed HA crystals shared the same orientation with their crystallographic c axis parallel to each other; and they were perpendicular to the dentin surface to form enamel-like structure (Figure 4 i and j).

Viewing from the transverse sections of the remineralized dentin slices, the dentinal tubules were gradually occluded by the precipitated HA crystals (d, f, h in Figure 4 and a, b in Figure 5). The dentinal tubules were occluded by the densely packed HA crystals after 6 cycles of mineralization. The precipitated HA crystals grew and became densely packed together to form bulk material. Some walls of the dentinal tubules were torn away during the process of preparing the transverse section samples.

Dentin collagen fibers are normally embedded and protected by HA (Figure 6 a). The HA can be removed and the dentin collagen fibers be exposed after acid-etching (Figure 6b). In this study, the demineralized dentin collagen matrix was remineralized and there was regeneration of the dentin microstructure of the calcified dentin collagen matrix after 2 cycles of mineralization (Figure 6 c) and resembling the natural dentin. Furthermore, the demineralized dentin collagen matrix was remineralized with intrafibrillar and interfibrillar HA formation (Figure 6 d, e and f). In some areas, the collagen fibers were remineralized with nano-HA particles precipitating along the collagen fibers to form a “string of beads” appearance, which corroborated intrafibrillar mineralization (Black arrow in Figure 6 d and f). The intrafibrillar mineralization was confirmed with the subsequent TEM examination.

Interfibrillar HA crystals were also formed with substantial mineralization. The spaces between the collagen fibrils were occupied by nano-crystals embedded between the collagen fibrils. A “corn-on-the-cob” appearance was found in some regions and finally making the collagen fibrils difficult to identify with the formation of interfibrillar HA (White arrow in Figure 6 d, e and f). A tight junction was observed at the interface between the precipitates in the dentinal tubules and the wall of the dentinal tubules (Figure 7). The precipitated HA particles were densely packed and adhered to the surface of the dentinal tubules.

3.3. TEM evaluation of intrafibrillar mineralization formation

The TEM bright-field micrographs showed remineralized dentin collagen fibrils after 6 cycles of mineralization (Figure 8a). The fibrils showed dark contrast, some discrete electron-dense islands, and some areas where the collagen fibrils were difficult to distinguish. The samples were not stained with phosphotungstic acid or any other electron-dense substance and these observations suggest the collagen fibrils were highly mineralized. Intrafibrillar mineralization of the collagen fibrils as well as interfibrillar mineralization of the matrix adjacent to the fibrils was found in the electron-dense images (Figure 8 b). SAED pattern of the precipitates revealed discrete string-like patterns that were characteristic of HA (Figure 8 c) The EDS spectrum shows presence of calcium, phosphate, and oxygen in the remineralized collagen fibrils (Figure 8 d). In contrast, the TEM micrograph of dentin collagen fibrin in demineralized dentin was hazy and indistinct (Figure 8e). There is no arch or ring image in SAED pattern (Figure 8 f).

4. DISCUSSION

4.1 The contribution of electric field to the regeneration of tooth-like tissue structure in the agarose hydrogel model

Collagen fibrils are the basic building blocks of mineralized dentin. It is therefore essential to understand its role in biomineralization. However, the function of collagen in the mechanism of hard tissues biomineralization remains unclear. Studies reported that the collagen matrix can serve as a scaffold for crystal deposition although it does not have the capacity to induce matrix-specific mineral formation from metastable calcium phosphate solutions.[32, 33] As a result, much attention has been paid to the non-collagenous proteins (NCPs), which have a high affinity for calcium ions and collagen fibrils. Moreover, NCPs are responsible for regulating the nucleation and growth of the mineral phase in mineralized hard tissues. Many studies have focused on investigating the promoting effects of biomimetic analogs of NCPs on crystal nucleation and crystal growth.[14, 16, 24, 34, 35] Several *in vitro* studies have demonstrated that ordered mineralization of apatite inside collagen fibrils is impossible without biomimetic analog additives.[36, 37] On the other hand, some *in vitro* studies showed that

type I collagen can initiate and orientate the growth of carbonated apatite mineral in the absence of any other extracellular matrix molecules from vertebrate calcified tissues. Furthermore, collagen matrix can influence the structural characteristics at the atomic scale and control the size and the three-dimensional distribution of apatite at larger length scales.[37, 38] In this study, a novel electrophoresis-aided biomineralization system is successfully developed t to induce dentin matrix remineralization without biomimetic NCP analogs. Results of SEM showed that the precipitated particles were regularly and homogenously distributed along the collagen fibrils in a "string of beads" structure in the dentin collagen matrix. This observation suggested the intrafibrillar mineralization of the dentin collagen matrix. Intrafibrillar mineralization could also be identified with TEM.

Furthermore, there was substantial mineral growth exhibiting a ''corn-on-the-cob'' appearance due to the connections between the remineralized collagen fibrils. This pattern suggested interfibrillar mineralization. It is suggested that the intrafibrillar mineralization might act as apatite seed crystallites to facilitate the growth of nano-crystals along the collagen fibril, resulting in ongoing mineral buildup on the exterior and the formation of interfibrillar mineralization. The HA nano-crystals grew and became connected to the mineralized intrafibrillar collagen fibrils. Our previous study showed agarose gel loaded with calcium and phosphate ions alone was not able to induce interfibrillar mineralization.[7] The function of the electric current in inducing the formation of interfibrillar mineralization is important in this electrophoresis-aided biomineralization system.

There are several advantages of the electrophoresis-aided biomineralization system. Firstly, hard tissue mineralization naturally occurs under a unique gel-like organic matrix. To mimic the gel-like microenvironment, a hydrogel-based biomimetic mineralization model using agarose gel loaded with calcium and phosphate ions was developed. The mode of crystal growth is different than that in aqueous solutions in the gel-like micro-environment. The physio-chemical nature of the gel-like micro-environment is more realistically mimics the unique mineralized tissue matrix environment than that of the aqueous solutions.

Numerous pores with diameter in the range of nanometer to micrometer are present in hydrogel. The porous structure of hydrogel allows diffusion of the crystallization solution in and out of the scaffold; and the pores act as the compartmentalized areas to regulate the nucleation and growth of the mineral phase in mineralizing process. The property of agarose hydrogel also make it favorable as biomimetic mineralization templates.[39] The restricted space in the gel network may entail a uniform and controllable size and structure on the precipitated HA. Our pervious study demonstrated that nanoscale, complex amorphous calcium phosphate precursors could be formed in the agarose hydrogel.[40] Kamitakahara et al. reported that the size of the HA granules could be controlled by the concentration of the hydrogel.[41]

Secondly, applying an electric field has a critical role in promoting the bioremineralization. The current accelerates the speed of migration of the calcium and phosphate ions in the agarose hydrogel. Moreover it can impose a specific direction of ions migration. Calcium and phosphate can be directed to flow easily in hydrogel.[29, 30, 41] In this electrophoresis-aided biomineralization system, the rate of mineral deposition on dentine slice is faster than that with traditional diffusion system. A 'cloud' of white suspension was formed in the agarose hydrogel after the current was applied (Figure 9). It became larger and denser with time, and reached its maximum size after 2 hours. In this study, the hydrogel was refreshed every 2 hours which was defined as a cycle of mineralisation.

Watanabe and Akashi found that electrophoresis could be used to precipitate HA in an agarose gel to obtain a HA/agarose composite, and complete mineral formation was achieved in only 30 minutes when the electrophoresis was performed at 100 volts. They also demonstrated the precipitation of HA was accelerated by electrophoresis. The linear velocity of mineralizing areas was shown to be approximately 15 times greater than that of simple diffusion.[29] The electric current in the hydrogel enhanced movement of calcium and phosphate ions or mineral precursors to 'get in touch with' the collagen matrix. Therefore it not only facilitates intrafibrillar and interfibrillar mineralization, but also remineralization of peritubular and intertubular dentin collagen matrix. This may be the reason for inducing intrafibrillar and interfibrillar mineralization without adding NCPs or NCP analogs. In this study, the results

corroborates that electrophoresis fosters the induction of intrafibrillar and interfibrillar mineralization and to accelerating the speed of remineralization. Furthermore, precipitation of HA was uneven on the dentin surface and the rate of precipitation varied in at different areas of the dentin slice. This might be due to variation of the electric resistance in different areas of the dentin slice, and thus the electric current varied at different areas of the slice. As a result, the concentration of calcium and phosphate were not the same at different areas of the slice. Pilot study was performed in this electrophoresis-aided calcium and phosphate hydrogel system and the results showed that 20 mA is adequate for the electrophoresis. Increasing the amount of electric current applied in the system had no significant change in both the rate of HA precipitation and morphology of the precipitates.

4.2 The ideal self-healing strategy for dentin

Dentine hypersensitivity is becoming more prevalent among patients and erosive wear is now an important clinical condition for clinician to manage.[42,43] This study provides an alternative strategy through biomimetic mineralization for clinical management of non-carious tooth loss with exposure of dentin. Exposing dentin of a tooth to acidic food and beverage causes dentin demineralization. The loss of HA would expose the dentin organic matrix (which composed mainly of type I collagen) to the oral environment and therefore results in breakdown of the collagen fibrils. As above mentioned, calcified collagen fibrils, especially the intrafibrillar mineralization of collagen fibrils, are responsible for the biomechanical properties of dentin and protecting collagen fibers from degradation.[42,13] Thus, through remineralizing the collagen fibrils to regenerate the dentin microstructure, this strategy should have great significance in clinical management. In this study, demineralized collagen matrix was remineralized with the formation of intrafibrillar and interfibrillar HA crystallites, resulting in the duplication of the dentin microstructure containing calcified collagen fibrils.

Exposing dentin to the oral environment often causes dentin hypersensitivity. Numerous pores which are openings of dentinal tubules are found on dentin surface. Local environment changes, such as temperature, pressure, osmolality, and chemical agents, cause movement of fluids in the dentinal tubules. This would stimulate the underlying nerves

surrounding the odontoblasts in dental pulp and give rise to pain, as postulated in the hydrodynamic theory. A common strategy to manage dentin hypersensitivity is to occlude the openings of dentinal tubules using dentin bonding agents, desensitizing toothpastes, laser therapy and even dental restoration.[43] However, these treatments have their considerable limitations.[44] Using this novel electrophoresis-aided biomineralization system, the HA precipitates almost completely occluded the dentinal tubules. In addition, the HA precipitates grew from the walls of the dentinal tubules and probably firmly adhere to the dentinal tubules. The precipitates also have the similar crystal structure to that of the natural tooth, and conceivably a similar coefficient of expansion. This is a favorable factor that contributes to its longevity of adhesion of the HA precipitate to dentin.

Natural dentin is covered by a layer of enamel or cementum which provides protection of the dentin-pulp complex from external stimuli or assaults. In this study, we successfully regenerated a layer of enamel-like tissue that grew from the remineralized dentin collagen matrix. There are few studies in the literature reporting the regeneration of enamel-like tissue from remineralized dentin collagen matrix. Through this mineralizing protocol, we are able to regenerate dentin microstructure of calcified collagen matrix, occlude the dentinal tubules, and create a layer of enamel-like tissue to cover the remineralized dentin surface. Furthermore, this novel electrophoresis-aided biomineralization system make use of electric current to shorten the time required for the HA precipitation. Further studies can be conducted to utilize this strategy for clinical management of dentin hypersensitivity.

5. CONCLUSION

A novel system utilizing electrophoresis to facilitate biomineralization system was successfully developed. This electrophoresis-aided biomineralization system contains calcium and phosphate-loaded agarose hydrogels without the addition of biomimetic NCP analogs. The system can induce remineralization of the dentin collagen matrix by formation of intrafibrillar and interfibrillar HA crystallites to generate dentin microstructure of calcified collagen fibrils. The HA crystals formed occludes the dentinal tubules. This novel electrophoresis-aided

biomineralization system regenerates enamel-like tissue on the dentin surface, and thus can be a good strategy to treat dentin defects and manage dentin hypersensitivity.

DISCLOSURE

The authors declare no competing financial interest.

ACKNOWLEDGMENT

This project was supported by NSFC/RGC Joint Research Scheme (N_HKU 776/10 and No.81061160511) and NSFC Grant (No. 30973352).

REFERENCES

1. Chen, H.; Tang, Z.; Liu, J.; Sun, K.; Chang, S. R.; Peters, M. C.; Mansfield, J. F.; Czajka‐Jakubowska, A.; Clarkson, B. H., *Advanced Materials* **2006,** *18* (14), 1846-1851.
2. Yamagishi, K.; Onuma, K.; Suzuki, T.; Okada, F.; Tagami, J.; Otsuki, M.; Senawangse, P., *Nature* **2005,** *433* (7028), 819-819.
3. Chen, H.; Clarkson, B. H.; Sun, K.; Mansfield, J. F., *Journal of colloid and interface science* **2005,** *288* (1), 97-103.
4. Fowler, C. E.; Li, M.; Mann, S.; Margolis, H. C., *Journal of Materials Chemistry* **2005,** *15* (32), 3317-3325.
5. Xie, R.; Feng, Z.; Li, S.; Xu, B., *Crystal growth & design* **2011,** *11* (12), 5206-5214.
6. Li, L.; Mao, C.; Wang, J.; Xu, X.; Pan, H.; Deng, Y.; Gu, X.; Tang, R., *Advanced Materials* **2011,** *23* (40), 4695-4701.
7. Fan, Y.; Sun, Z.; Moradian-Oldak, J., *Biomaterials* **2009,** *30* (4), 478-483.
8. Fan, Y.; Wen, Z. T.; Liao, S.; Lallier, T.; Hagan, J. L.; Twomley, J. T.; Zhang, J.-F.; Sun, Z.; Xu, X., *Journal of bioactive and compatible polymers* **2012,** *27* (6), 585-603.
9. Ruan, Q.; Zhang, Y.; Yang, X.; Nutt, S.; Moradian-Oldak, J., *Acta biomaterialia* **2013,** *9* (7), 7289-7297.
10. Busch, S., *Angewandte Chemie International Edition* **2004,** *43* (11), 1428-1431.
11. Liu, S.; Yin, Y.; Chen, H., *CrystEngComm* **2013,** *15* (29), 5853-5859.
12. Balooch, M.; Habelitz, S.; Kinney, J.; Marshall, S.; Marshall, G., *Journal of structural biology* **2008,** *162* (3), 404-410.
13. Carrilho, M. R. d. O.; Tay, F. R.; Pashley, D. H.; Tjäderhane, L.; Marins Carvalho, R., *Dental Materials* **2005,** *21* (3), 232-241.
14. Tay, F. R.; Pashley, D. H., *Biomaterials* **2008,** *29* (8), 1127-37.
15. He, G.; Dahl, T.; Veis, A.; George, A., *Connective tissue research* **2003,** *44* (1), 240-245.
16. He, G.; George, A., *Journal of Biological Chemistry* **2004,** *279* (12), 11649-11656.
17. He, G.; Dahl, T.; Veis, A.; George, A., *Nature materials* **2003,** *2* (8), 552-8.
18. Rahiotis, C.; Vougiouklakis, G., *Journal of dentistry* **2007,** *35* (8), 695-698.
19. Rahiotis, C.; Vougiouklakis, G.; Eliades, G., *Journal of dentistry* **2008,** *36* (4), 272-80.

20. Mitchell, J. C.; Musanje, L.; Ferracane, J. L., *Dental materials : official publication of the Academy of Dental Materials* **2011,** *27* (4), 386-93.

21. Zhou, Y. Z.; Cao, Y.; Liu, W.; Chu, C. H.; Li, Q. L., *ACS Appl.Mater interfaces* **2012,** *4* (12), 6901-10.

22. Ning, T. Y.; Xu, X. H.; Zhu, L. F.; Zhu, X. P.; Chu, C. H.; Liu, L. K.; Li, Q. L., *Journal of Biomedical Materials Research Part B: Applied Biomaterials* **2012,** *100* (1), 138-144.

23. Niu, L. N.; Zhang, W.; Pashley, D. H.; Breschi, L.; Mao, J.; Chen, J. H.; Tay, F. R., *Dental materials : official publication of the Academy of Dental Materials* **2014,** *30* (1), 77-96.

24. Cao, Y.; Mei, M. L.; Xu, J.; Lo, E. C.; Li, Q.; Chu, C. H., *Journal of dentistry* **2013,** *41* (9), 818-25.

25. Cao, Y.; Liu, W.; Ning, T.; Mei, M. L.; Li, Q.-L.; Lo, E. C.; Chu, C., *Clin Oral Investig* **2013**, 1-9.

26. Wang, Q.; Wang, X.; Tian, L.; Cheng, Z.; Cui, F., *Soft Matter* **2011,** *7* (20), 9673-9680.

27. Burwell, A. K.; Thula-Mata, T.; Gower, L. B.; Habelitz, S.; Kurylo, M.; Ho, S. P.; Chien, Y. C.; Cheng, J.; Cheng, N. F.; Gansky, S. A.; Marshall, S. J.; Marshall, G. W., *PloS one* **2012,** *7* (6), e38852.

28. Li, J.; Yang, J.; Li, J.; Chen, L.; Liang, K.; Wu, W.; Chen, X.; Li, J., *Biomaterials* **2013**.

29. Watanabe, J.; Akashi, M., *Biomacromolecules* **2006,** *7* (11), 3008-3011.

30. Watanabe, J.; Kashii, M.; Hirao, M.; Oka, K.; Sugamoto, K.; Yoshikawa, H.; Akashi, M., *J Biomed Mater Res A* **2007,** *83* (3), 845-52.

31. Cao, Y.; Mei, M. L.; Li, Q. L.; Lo, E. C.; Chu, C. H., *ACS Appl.Mater interfaces* **2014,** *6* (1), 410-20.

32. Saito, T.; Arsenault, A.; Yamauchi, M.; Kuboki, Y.; Crenshaw, M., *Bone* **1997,** *21* (4), 305-311.

33. Saito, T.; Yamauchi, M.; Abiko, Y.; Matsuda, K.; Crenshaw, M. A., *Journal of Bone and Mineral Research* **2000,** *15* (8), 1615-1619.

34. Kim, J.; Arola, D. D.; Gu, L.; Kim, Y. K.; Mai, S.; Liu, Y.; Pashley, D. H.; Tay, F. R., *Acta biomaterialia* **2010,** *6* (7), 2740-50.

35. Kim, Y. K.; Gu, L. S.; Bryan, T. E.; Kim, J. R.; Chen, L.; Liu, Y.; Yoon, J. C.; Breschi, L.; Pashley, D. H.; Tay, F. R., *Biomaterials* **2010,** *31* (25), 6618-27.

36. Nudelman, F.; Pieterse, K.; George, A.; Bomans, P. H.; Friedrich, H.; Brylka, L. J.; Hilbers, P. A.; Sommerdijk, N. A., *Nature materials* **2010,** *9* (12), 1004-1009.

37. Silver, F. H.; Landis, W. J., *Connective tissue research* **2011,** *52* (3), 242-254.

38. Wang, Y.; Azais, T.; Robin, M.; Vallee, A.; Catania, C.; Legriel, P.; Pehau-Arnaudet, G.; Babonneau, F.; Giraud-Guille, M. M.; Nassif, N., *Nature materials* **2012,** *11* (8), 724-33.

39. Munro, N. H.; McGrath, K. M., *Bioinspired, Biomimetic and Nanobiomaterials* **2012,** *1* (1), 26-37.

40. Guentsch, A.; Busch, S.; Seidler, K.; Kraft, U.; Nietzsche, S.; Preshaw, P. M.; Chromik, J. N.; Glockmann, E.; Jandt, K. D.; Sigusch, B. W., *Adv Eng Mater* **2010,** *12* (9), B571-B576.

41. Kamitakahara, M.; Kimura, K.; Ioku, K., *Colloids and Surfaces B: Biointerfaces* **2012,** *97*, 236-239.

42. Balooch, M.; Habelitz, S.; Kinney, J.; Marshall, S.; Marshall, G., *J Struct Biol* **2008,** *162* (3), 404-410.

43. Chu, C.; Lam, A.; Lo, E., *General dentistry* **2011,** *59* (2), 115.

44. Bakry, A. S.; Tamura, Y.; Otsuki, M.; Kasugai, S.; Ohya, K.; Tagami, J., *Journal of dentistry* **2011,** *39* (9), 599-603.

485

Table of Contents

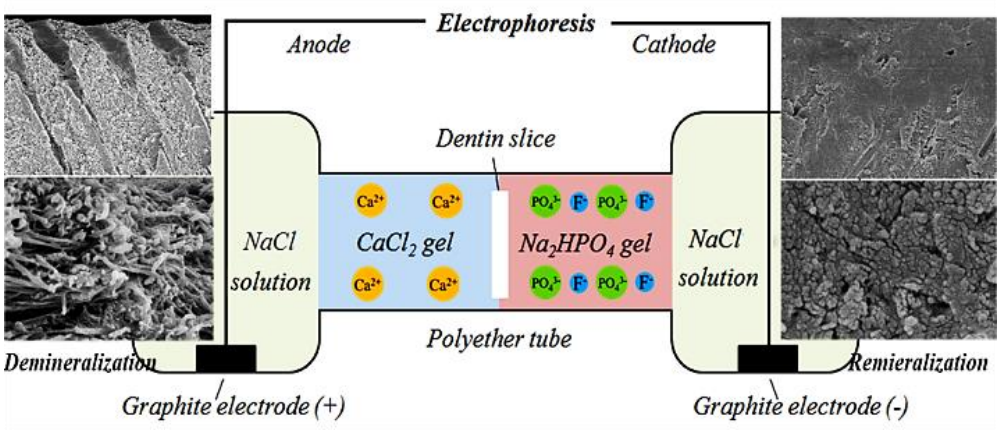

486

Figure 1. Schematic diagram of the electrophoresis aided calcium and phosphate hydrogel system

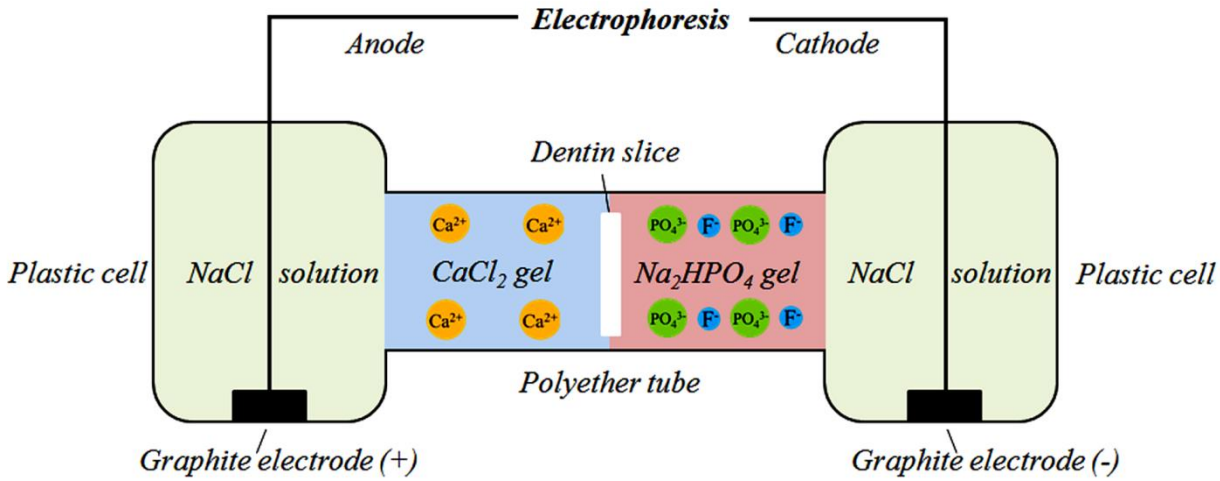

Figure 2. XRD spectrum of the precipitates on dentin after 6 cycles of mineralization

Precipitates from (a – red line) electrophoresis, (b – black line) dentin without acid-etching, and (c – blue line) acid-etched dentin.

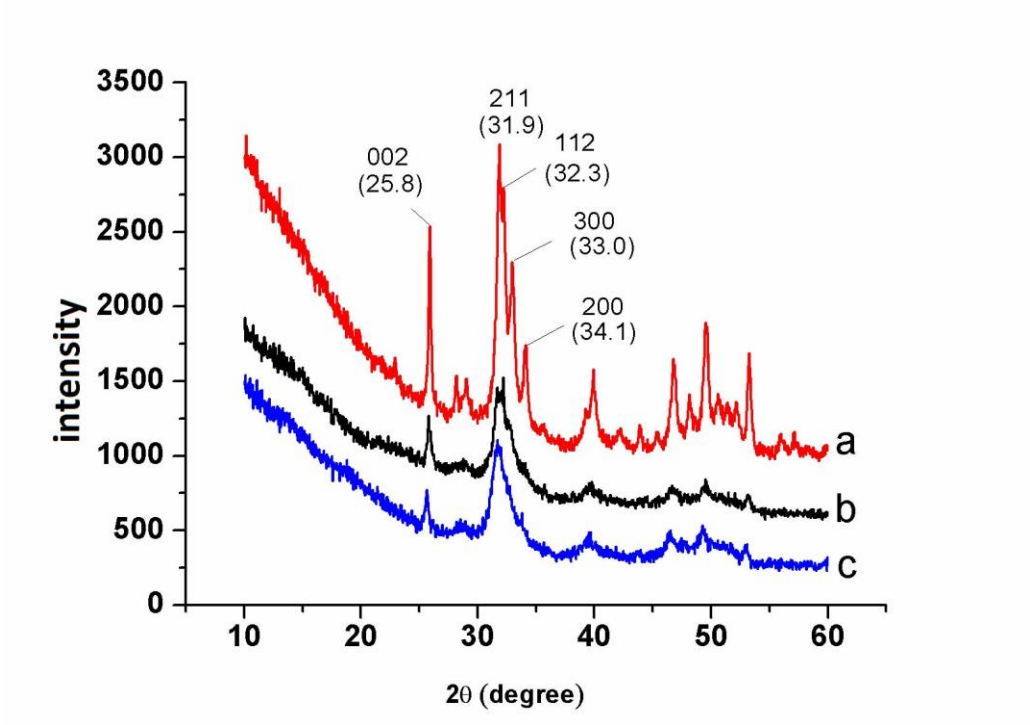

Figure 3. FTIR spectrum of the precipitates on dentin after 6 cycles of mineralization

Precipitates from (a – red line) electrophoresis, (b – black line) dentin without acid-etching, and (c – blue line) acid-etched dentin.

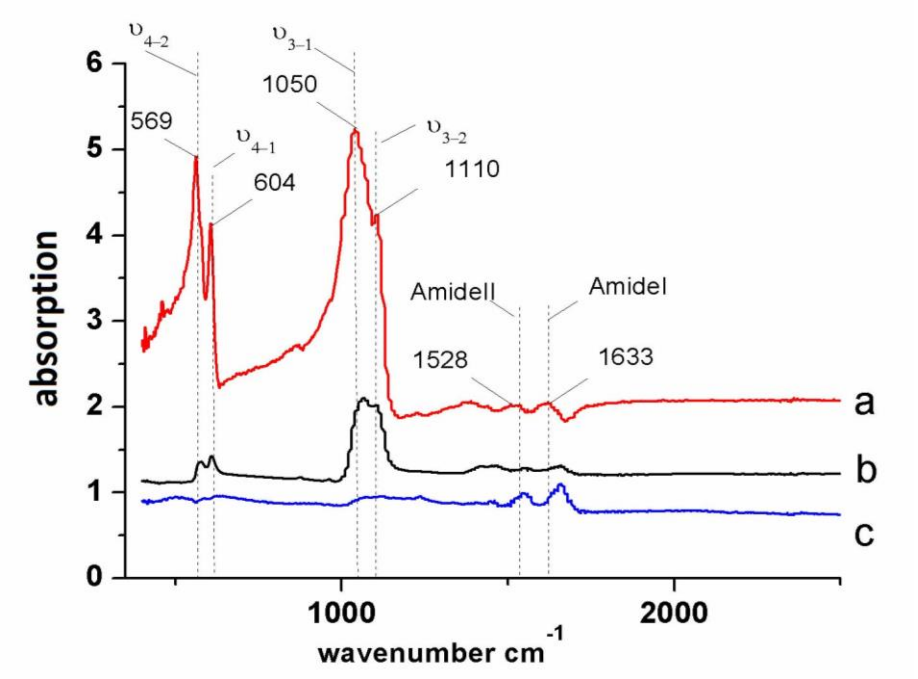

Figure 4. SEM micrographs of the remineralized dentin slices

(a, b) are dentin structures after acid-etching with 37% H_3PO_4 for 30s. (c, d), (e, f) and (g, h) are the samples of remineralization after 2, 4 and 6 mineralizing cycles, respectively. (b), (d), (f) and (h) are the cross-sectional views of the samples of (a), (c), (e) and (g) respectively. (i) - enamel after acid-etching with 37% H_3PO_4 for 30s showing the HA crystals with their c axis parallel to each other. (j) - the magnification of (g) showing the precipitated HA crystals orientation similar to (i). The micrographs showed needle-shaped HA crystals grew from the dentin surface and the wall of dentinal tubule, and gradually covered the dentinal surface and tubules to form enamel-like tissue.

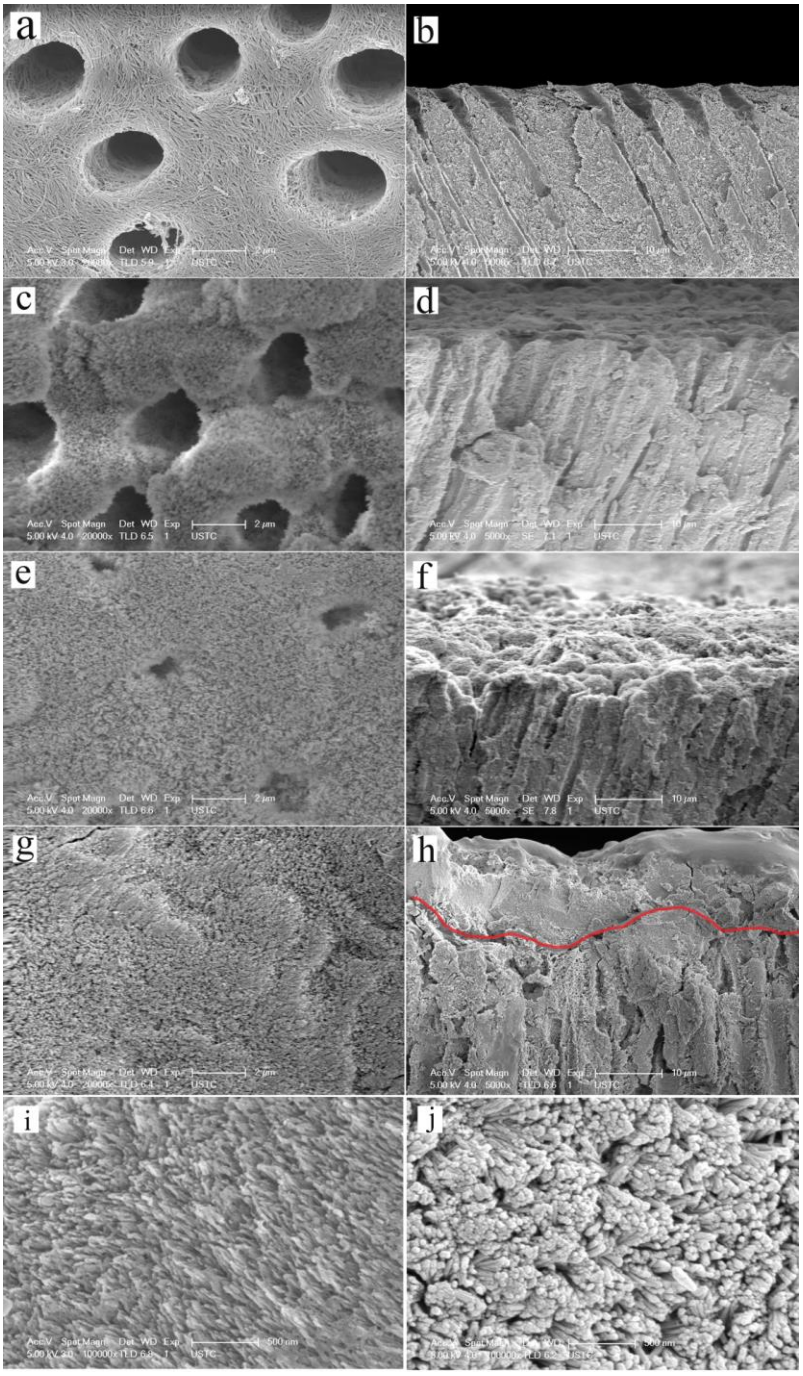

Figure 5. Dentin remineralization with occlusion of dentinal tubules

(a) and (b) - cross sections of the dentin slices after 2 and 6 mineralization cycles, respectively. (c) - magnified area of (b). (d) - natural dentinal tubule structure for comparison. Part of the wall of the dentinal tubules was torn away during preparation of the transverse section samples, and this suggested that the precipitated HA adhered firmly to the dentin structure (Figure 5 b).

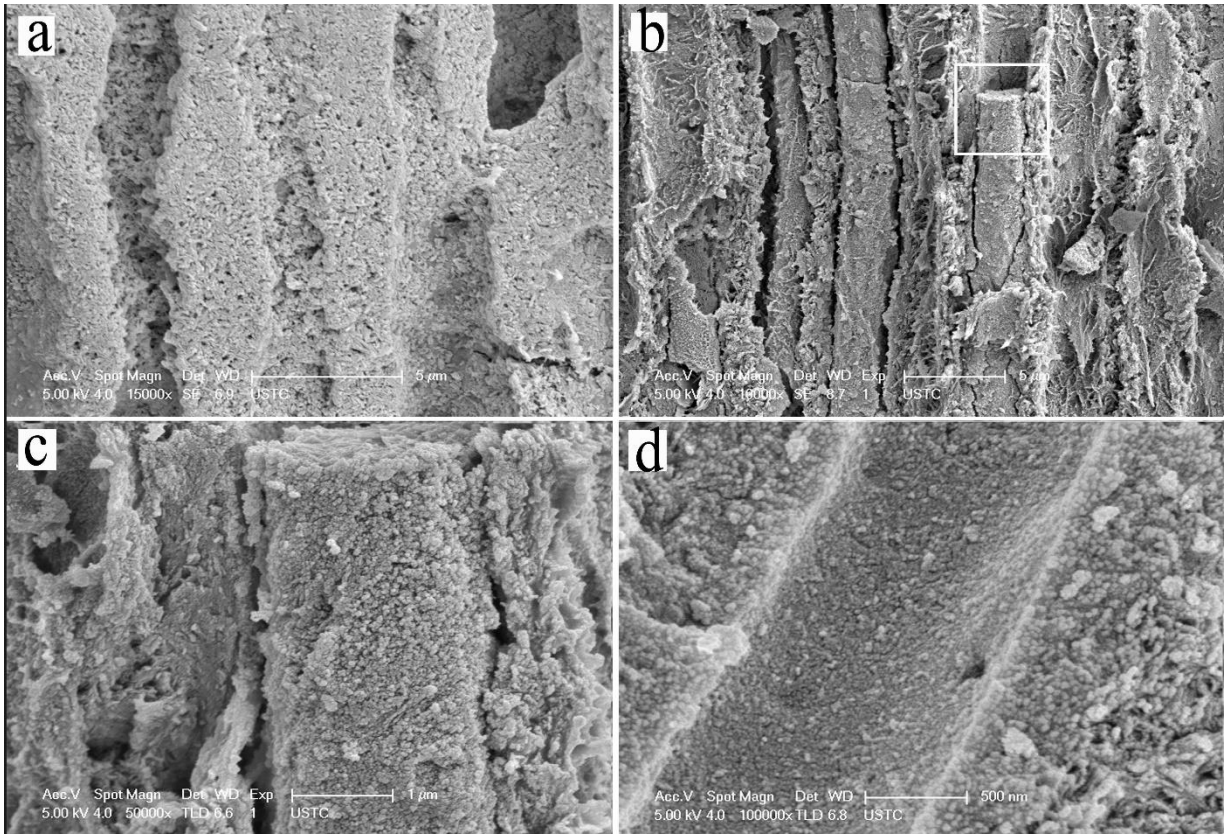

Figure 6. Dentin slices in cross-sections

(a) - natural dentin (b) – demineralized dentin collagen matrix after acid-etching. (c) - remineralized dentin collagen matrix after 2 cycles of remineralization. (d), (e) and (f) - remineralized collagen matrix showing the formation of intrafibrillar and interfibrillar HA in high magnification. The demineralized dentin collagen matrix was remineralized with the formation of intrafibrillar (black arrow) and interfibrillar HA (white arrow) to regenerate dentin microstructure.

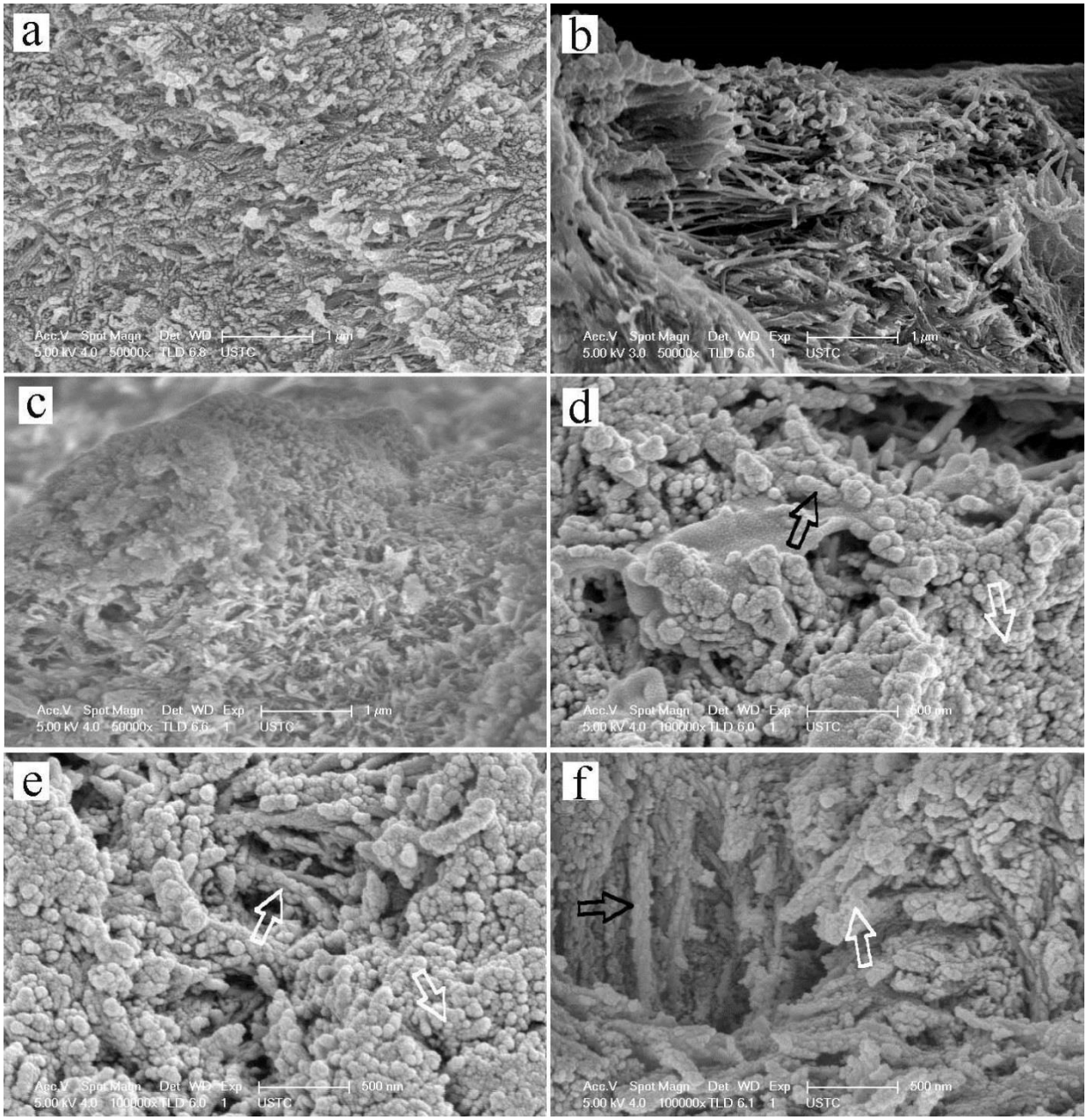

Figure 7. SEM micrographs showing interface between precipitates and the wall of the dentinal tubules of a remineralized dentin slice

(a) - remineralized dentin in cross-section. (b) – a magnified region of (a). (c) - the rectangular area of (b). (d) - the oval area of (b). The five-point star indicates remineralized dentin collagen matrix, the triangle star indicates precipitates in the dentinal tubules, and quadrangular star indicates precipitates on remineralized dentin collagen matrix surface. The interface of the HA precipitates and the underlying remineralized dentin was hardly distinguished (b, d), suggesting tight and strong binding of the precipitated HA crystals to dentin.

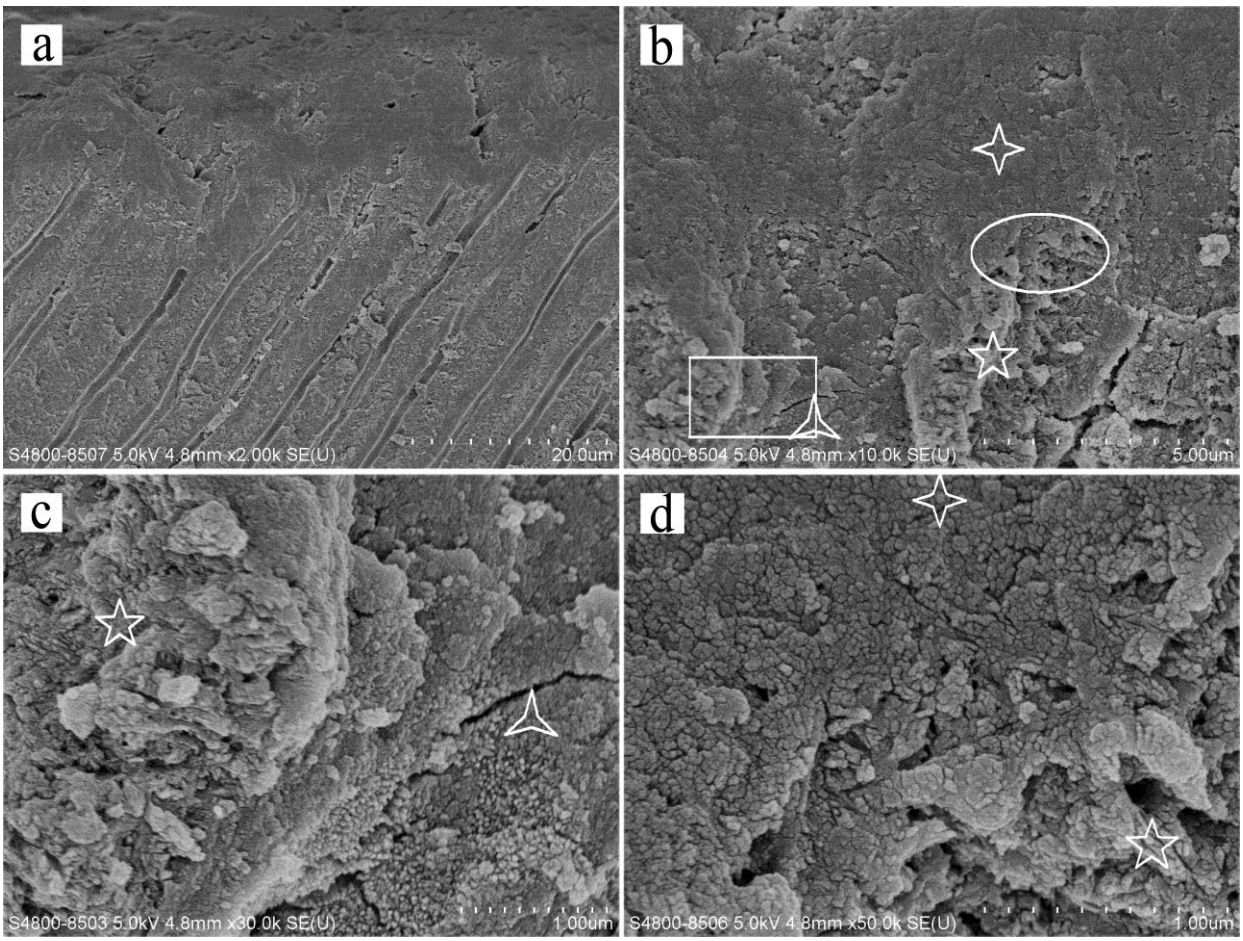

Figure 8. TEM micrographs of unstained remineralized dentin collagen fibrils

(a) - TEM bright-field micrograph of remineralized dentin collagen fibrils. (b) – magnified view of (a). (c) - SAED pattern of remineralized dentin collagen fibrils. (d) EDS spectra of remineralized dentin collagen fibrils. (e) TEM bright-field micrograph on demineralized dentin collagen fibrils of acid-etched dentin. (f) - SAED pattern of the demineralized dentin collagen fibrils.

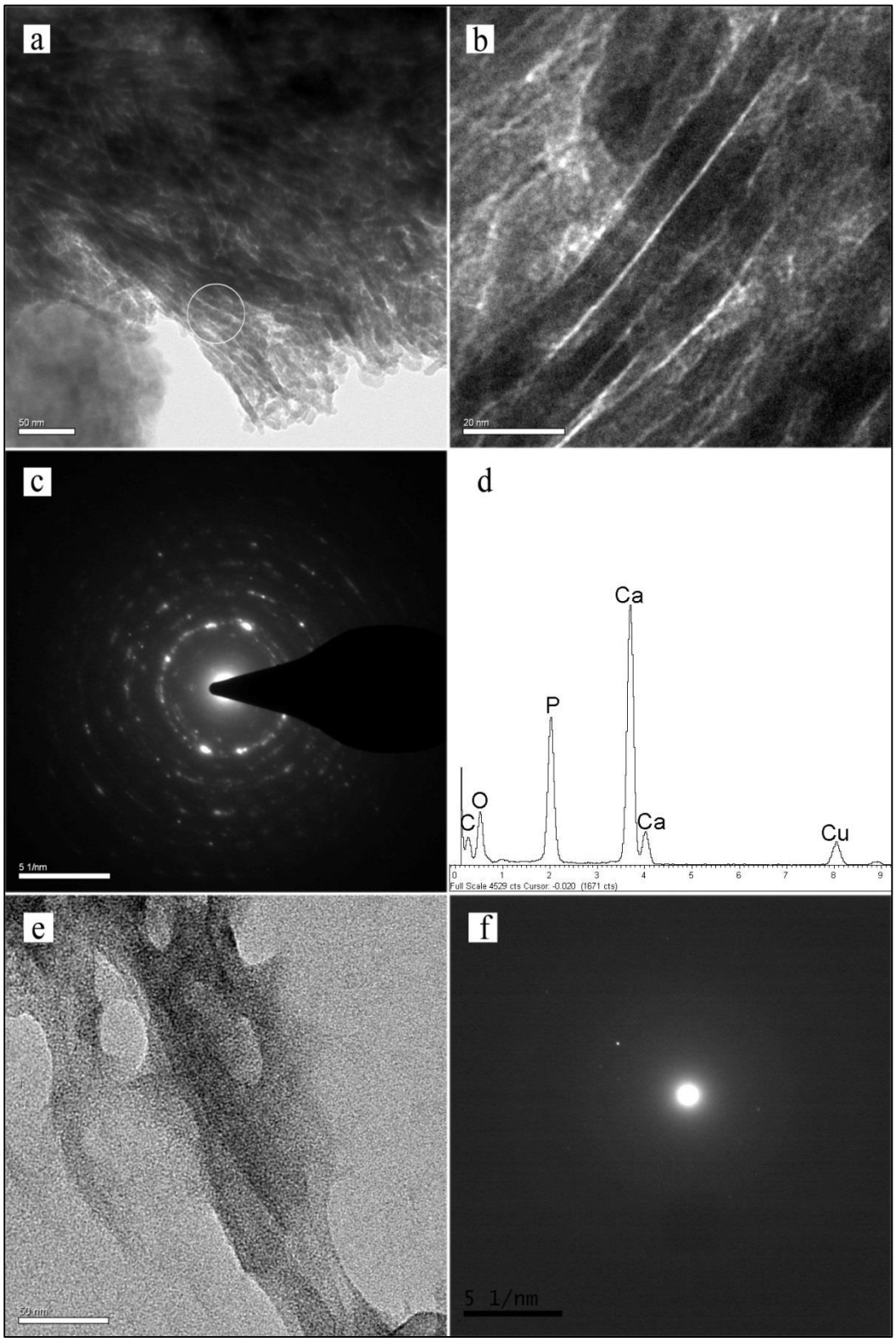
a
50 nm
b
20 nm
c
5 1/nm
d
Ca
P
O
C
Ca
Cu
0 1 2 3 4 5 6 7 8 9
Full Scale 4529 cts Cursor: -0.020 (1671 cts)
e
50 nm
f
5 1/nm

552
553

554 **Figure 9. Deposits formed on the dentin slice with time**

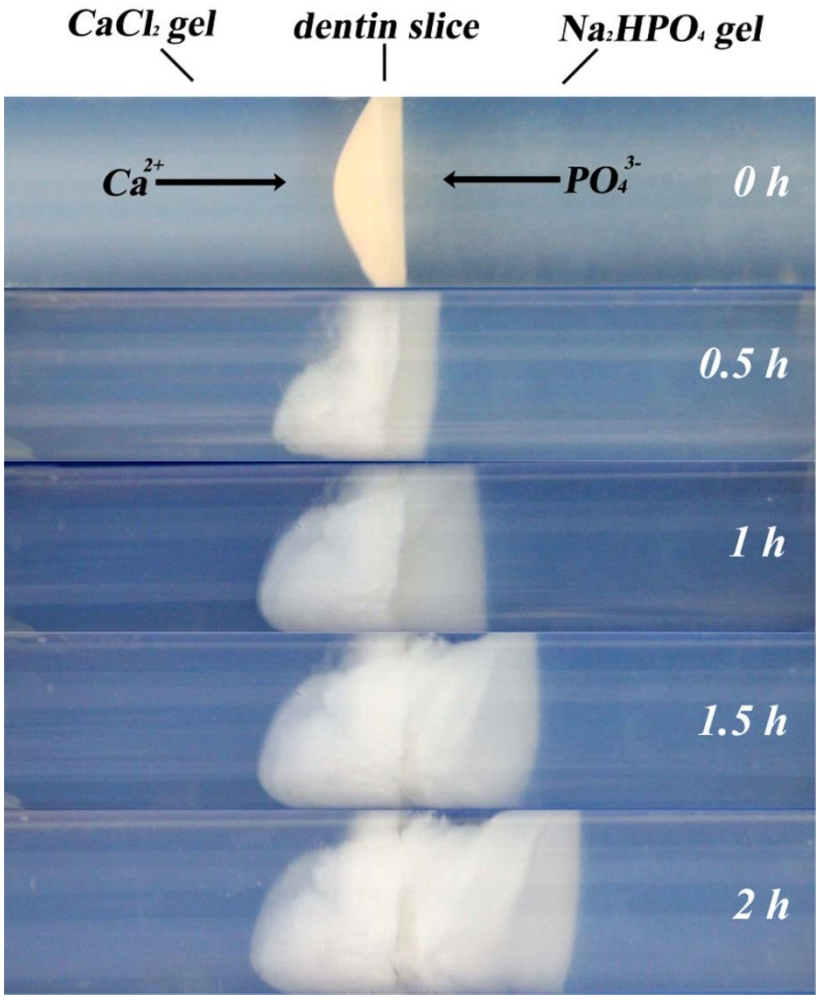

555

Figure10. The schematic diagram of the natural tooth structure and the regeneration of enamel prism-like tissue on demineralized dentin